R-05-39

Estimation of 3D positions and orientations of reflectors based on an updated interpretation of Stage 1 reflection seismic data

Preliminary site description Forsmark area – version 1.2

Lucian Balu, Calin Cosma
Vibrometric

May 2005

Svensk Kärnbränslehantering AB
Swedish Nuclear Fuel
and Waste Management Co
Box 5864
SE-102 40 Stockholm Sweden
Tel 08-459 84 00
+46 8 459 84 00
Fax 08-661 57 19
+46 8 661 57 19

ISSN 1402-3091
SKB Rapport R-05-39

Estimation of 3D positions and orientations of reflectors based on an updated interpretation of Stage 1 reflection seismic data

Preliminary site description Forsmark area – version 1.2

Lucian Balu, Calin Cosma
Vibrometric

May 2005

Abstract

Reflection seismic surveys were performed in the spring of 2002 in the Forsmark area. The 3D positions of the seismic reflectors derived by these surveys were subsequently computed and presented in a previous report during 2003. In 2004, a reinterpretation of the seismic data resulted in the identification of a few new reflectors and the reorientation of some that already existed in the previous model. The objective of this work was to update the 3D positions and orientations of these reflectors, prior to their use in the version 1.2, deformation zone modelling activity. A procedure aimed at converting the DMO representation to spatial dimensions was used. The procedure also included a reassessment of the velocity field. The main part of the present report describes the objectives, survey layout and results of the 3D positioning and orientation work. The methodology used, which is identical to that described in the earlier study, is extracted from the 2003 report and presented in Appendix 1. The seismic profiles are shown in Appendix 2.

Contents

1 Introduction

Reflection seismic surveys were performed in the spring of 2002 in the Forsmark area /Juhlin et al. 2002/. High-resolution seismic data were acquired along five profiles varying in length from 2 to 5 km. The 3D positions of the seismic reflectors derived by seismics were interpreted and presented in /Cosma et al. 2003/.

There were 25 reflectors originally derived by seismics. In 2004, a reinterpretation of the seismic data resulted in the identification of three new reflectors /Juhlin and Bergman, 2004/. Four of the ones already included in the site model were reoriented. These seven reflectors are listed in Table 1-1.

The main part of this report describes the objectives, survey layout and results of the 3D positioning work. The methodology used, which is identical to that described in /Cosma et al. 2003/, is extracted from this report and presented in Appendix 1. The seismic profiles are shown in Appendix 2.

Table 1-1. Reflectors added or modified in the updated interpretation.

Current No.	Reflector ID	Strike (º)	Dip (º)	Distance from origin (m)	Status
1	A7	55	23	–780	New
2	B6	30	32	–250	New
3	B7	25	20	1,700	New
4	A3	50	23	–50	Reoriented
5	B2	30	25	950	Reoriented
6	B3	30	21	1,750	Reoriented
7	D3	320	65	3,200	Reoriented

2 Objectives

The objective of this work was to update the interpretation reported in /Cosma et al. 2003/, bearing in mind the re-evaluation of the seismic data presented in /Juhlin and Bergman, 2004/. The reflecting segments are represented in all the figures of this report as plane elements with a transverse dimension of 100 m, which corresponds roughly to 3–4 signal wavelengths.

As in /Cosma et al. 2003/, a procedure aimed at converting the DMO representation to spatial dimensions was used (Appendix 1). The procedure included a reassessment of the velocity field. The present work included the computing of the orientations and extent of reflectors not visible throughout the profiles and/or visible as a sequence of articulated segments with different orientations.

3 Survey layout

Reflection seismic data were acquired along five profiles varying in length from 2 to 5 km. The investigation lines were not straight and, to apply the considerations given in Appendix 1, the investigation lines with significant deviations from linearity were split in several roughly linear parts as follows:

- Line 2 into line 2.1 (stations 1 to 325) and line 2.2 (stations 326 to 485).
- Line 5 into line 5.1 (stations 1 to 319), line 5.2 (stations 320 to 499) and line 5.3 (stations 500 to 979).

The investigation lines and nomenclature are shown in Figure 3-1. The start station on each profile is marked with a green dot.

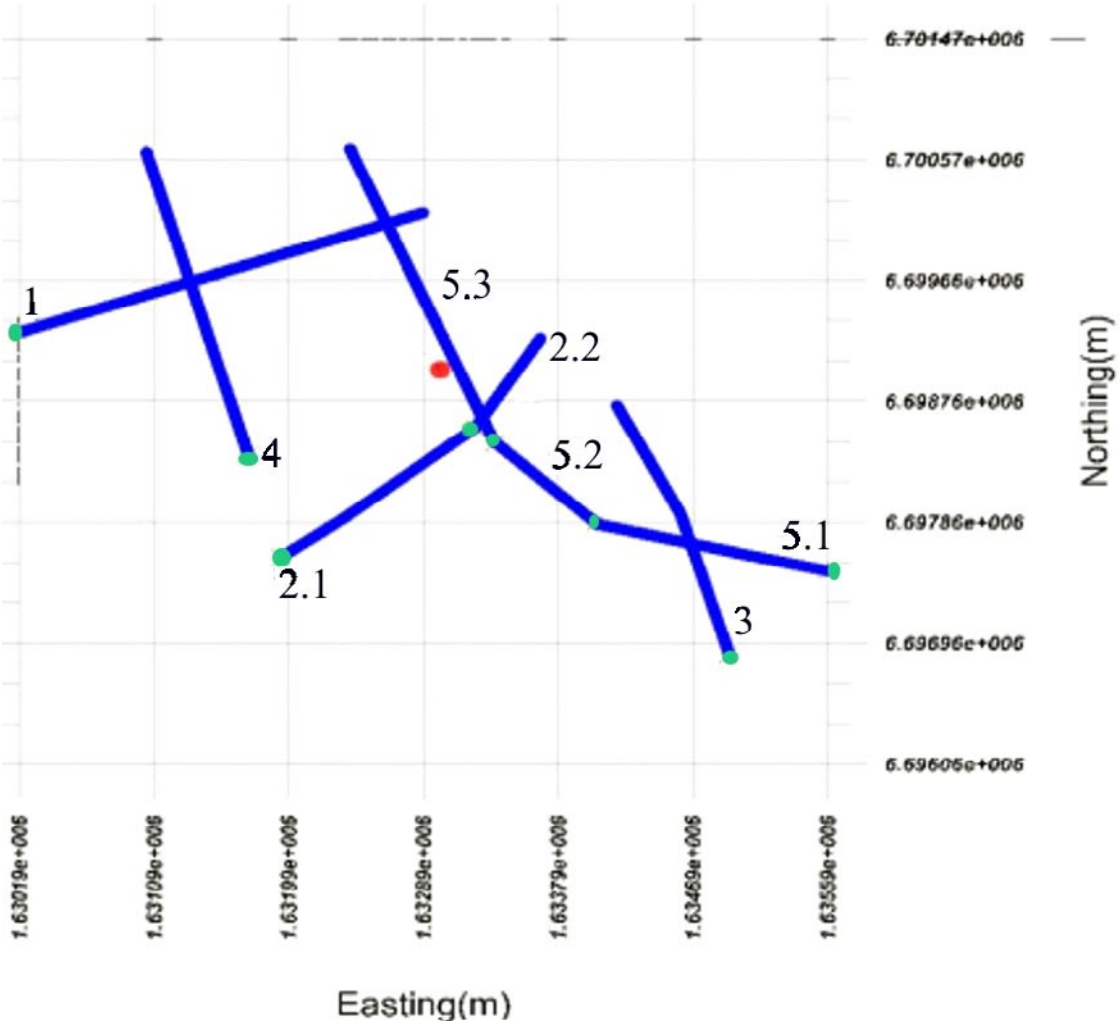

Figure 3-1. *Survey lines and nomenclature. Lines 2 and 5 are split into linear segments. The green dots represent the first station (lower ID) in each line segment. The red dot is the crux point origin at 6,699 km N, 1,633 km W.*

4 Results

The results of the geometrical reinterpretation of the Forsmark seismic reflectors A7, B6, B7, A3 are summarized in Table 4-1 and reflectors B2, B3, D3 in Table 4-2. Reflector A7 has been decomposed into two groups: one with the original dip and strike as presented in /Juhlin and Bergman, 2004/ (visible in 3 and 5.1), and the other group with the dip = 15 degrees (visible in 3 and 5.2).

For reflectors B2, B3, D3 the previous results are extracted from /Cosma et al. 2003/, since it was judged that there were no reasons to change the initial interpretation.

Table 4-1. Summary of orientations found for reflectors A7, B6, B7, A3.

Reflector ID	Dip (º)	Strike (º)	Dip (º)	Strike (º)	Azimuth (º)	Profile
A7	23	55	23	52	322	P3
			16	52	322	P3
			23	52	322	P5.1
			16	45	315	P5.2
B6	32	30	32	30	300	P3
			32	30	300	P5.1
B7	20	25	22	16	286	P1
			22	16	286	P5.3
A3	23	50	23	50	320	P3
			23	50	320	P5.1
			23	50	320	P5.2
			23	50	320	P5.3

Table 4-2. Summary of orientations found for reflectors B2, B3, D3.

Reflector ID	Original Dip (º)	Original Strike (º)	New Dip (º)	New Strike (º)	Visible in Profile	First station	Last station
B2	25	30	27	25	3	65	286
			27	25	5.1	68	319
B3	21	30	24	30	3	179	402
			24	30	5.1	111	319
D3	65	320	28	37	5.1	1	319
			28	37	3	1	402

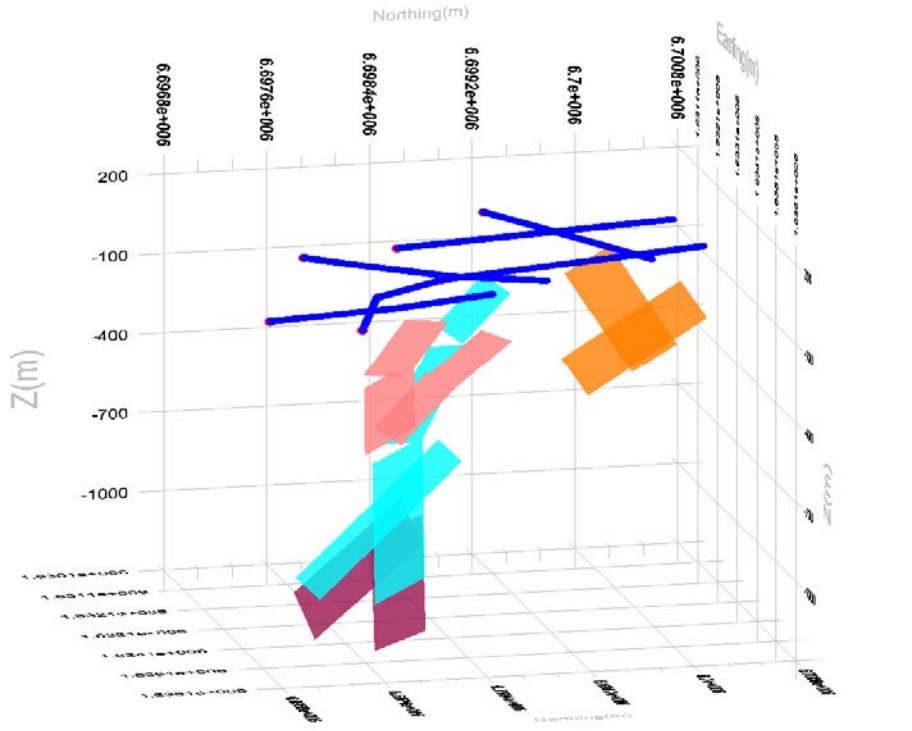

Figure 4-1. *Reflectors A7 (pink), B6 (red), B7 (orange), A3 (blue). View from east.*

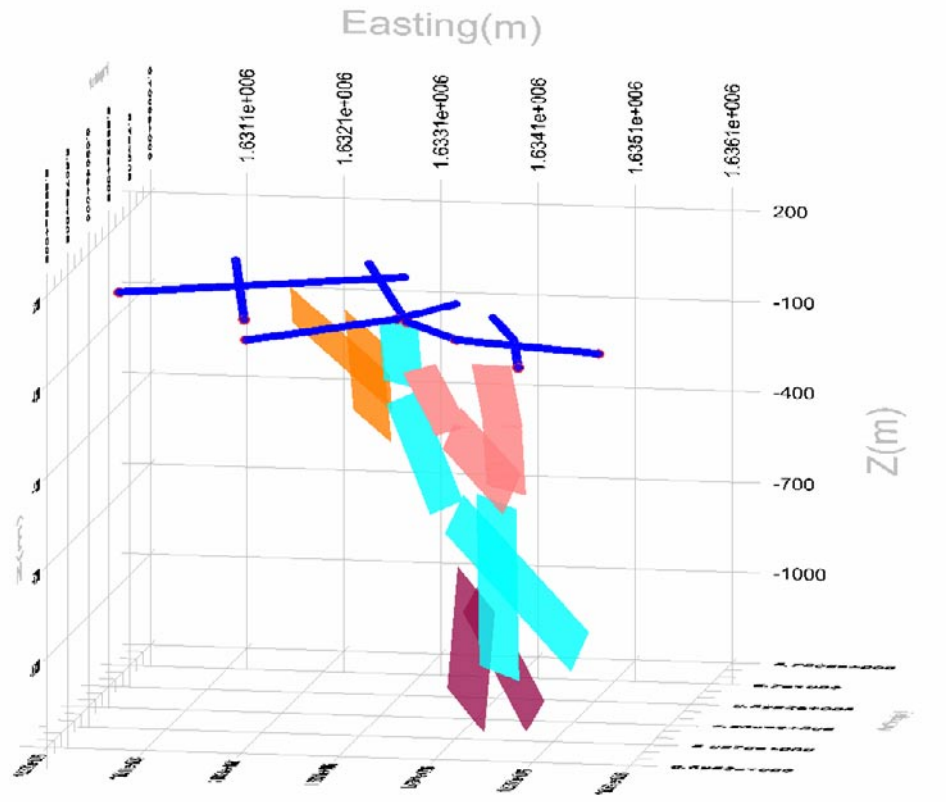

Figure 4-2. *Reflectors A7 (pink), B6 (red), B7 (orange), A3 (blue). View from south.*

Reflector A7 (N,E,Z)

Element from profile 3

6,697,934	1,634,734	–514.205
6,697,779	1,634,368	–469.584
6,698,202	1,634,212	–283.638
6,698,356	1,634,579	–328.259

Element from profile 3

6,698,356	1,634,589	–327.542
6,698,170	1,634,236	–307.521
6,698,675	1,633,979	–149.739
6,698,861	1,634,332	–169.76

Element from profile 5.1

6,698,071	1,634,111	–305.097
6,697,772	1,633,845	–311.615
6,698,167	1,633,398	–141.65
6,698,465	1,633,664	–135.131

Element from profile 5.2

6,698,052	1,634,653	–452.134
6,697,676	1,634,565	–557.263
6,697,770	1,633,920	–353.391
6,698,146	1,634,008	–248.262

Reflector B6 (N,E,Z)

Element from profile 3

6,698,099	1,634,879	–1,207.24
6,697,715	1,634,793	–1,280.29
6,697,792	1,634,124	–894.088
6,698,176	1,634,210	–821.044

Element from profile 5.1

6,697,302	1,634,474	–1,251.18
6,697,193	1,634,122	–1,094.99
6,698,041	1,634,005	–766.711
6,698,150	1,634,357	–922.903

Reflector B7 (N,E,Z)

Element from profile 1

6,700,017	1,631,752	–28.6229
6,699,647	1,631,875	–117.586
6,700,028	1,632,796	–433.777
6,700,399	1,632,673	–344.814

Element from profile 5.3

6,699,521	1,632,533	–387.996
6,699,675	1,632,882	–506.826
6,700,654	1,632,533	–261.796
6,700,500	1,632,184	–142.966

Reflector A3 (N,E,Z)

Element from profile 3

6,697,154	1,634,462	–1,014.28
6,697,287	1,634,835	–1,073.02
6,698,445	1,634,498	–604.299
6,698,313	1,634,125	–545.562

Element from profile 5.1

6,697,642	1,635,272	–1,068.36
6,698,020	1,635,357	–968.749
6,698,210	1,634,015	–541.046
6,697,832	1,633,930	–640.657

Element from profile 5.2

6,698,609	1,633,492	–237.075
6,698,445	1,633,130	–191.538
6,698,840	1,632,972	–20.1136
6,699,004	1,633,334	–65.6507

Element from profile 5.3

6,697,896	1,633,751	–584.527
6,698,194	1,634,017	–560.163
6,698,686	1,633,437	–242.021
6,698,388	1,633,171	–266.384

References

Cosma C, Balu L, Enscu N, 2003. Estimation of 3D positions and orientations of reflectors identified in the reflection seismic survey at the Forsmark area. SKB R-03-22, Svensk Kärnbränslehantering AB.

Juhlin C, Bergman B, 2004. Reflection seismics in the Forsmark area. Updated interpretation of Stage 1 (previous report R-02-43). Updated estimate of bedrock topography (previous report P-04-99). SKB P-04-158, Svensk Kärnbränslehantering AB.

Juhlin C, Bergman B, Palm H, 2002. Reflection seismic studies in the Forsmark area – stage 1. SKB R-02-43, Svensk Kärnbränslehantering AB.

Appendix 1

Methodology (extracted from /Cosma et al. 2003/)

DMO representation and reflector positioning

The DMO (dip moveout) procedure is used to compensate for time stretches due to variable source-receiver offsets. After DMO, reflection onsets on different traces originating at the same point in space are brought to the same time mark and can therefore be stacked. The horizontal axis of a DMO profile is the distance along the measured seismic line. However, the vertical axis is still time, not depth. To transfer the representation from X-t (distance-time) to X-R (distance-depth) coordinates, one must first consider a velocity field. R, rather than Z is taken here to represent the depth, as there is no reason to assume a priori that reflectors are positioned vertically beneath the seismic line. Let a constant velocity V=const. be considered. In Figure A1-1, a reflection event picked at A1 on trace S1 can arrive from any reflector tangent to the sphere with the center in S1 and the radius R1=V·t1/2. Likewise, a reflection event picked at time A2 on trace S2 can arrive from any reflector tangent to the sphere with the center in S2 and the radius R2=V·t2/2.

Let us assume that the segment A1A2 is picked in the X-t data profile along a visible reflection event extending from trace S1 to trace S2. The corresponding reflection segment in the X-R space is B1B2, which is a tangent to the two spheres with diameters R1 and R2. The dip and position errors are negligible for deep sub-horizontal reflectors where R1~R2 but may become significant for steep and/or shallow reflectors where R1 # R2. By simple geometrical considerations it can be proven that the intersection point with the surface

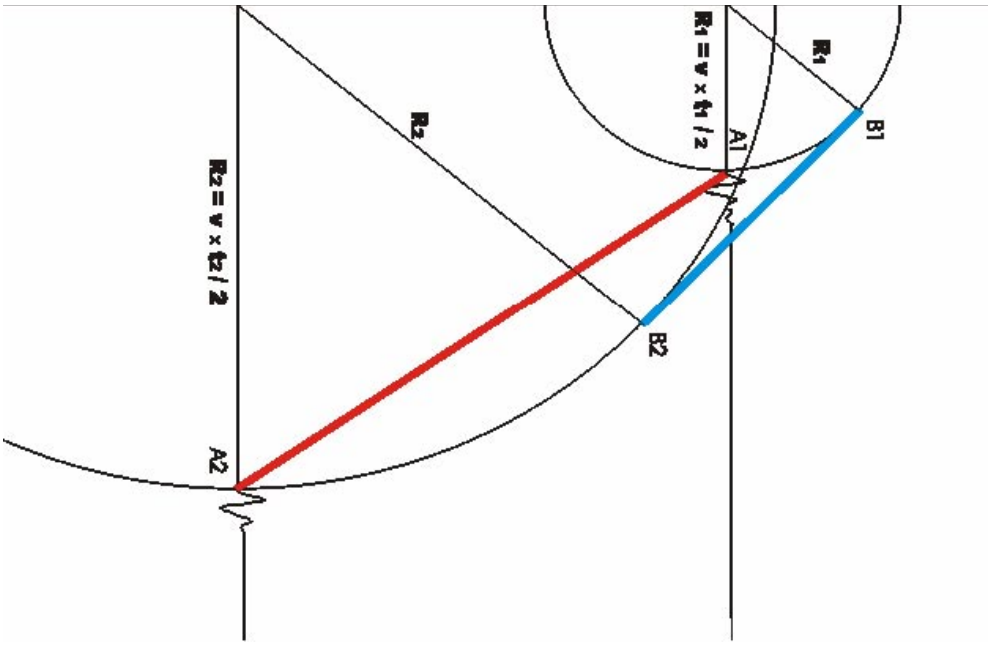

Figure A1-1. *Schematic representation of a DMO-corrected profile. The survey line runs horizontally. The vertical axis is the time to the reflector, which becomes distance to the reflector by taking d=t·v/2 with v=const. The distance is the same with the vertical depth only for horizontal reflectors. Dipping reflectors lining with the segment A1A2 in the DMO profile are actually located along B1B2, i.e. tangent to the spheres with the centers in S1 and S2 and the radii R1=t1·v /2 R2=t2·v /2.*

is the same for A1A2 and any realization of B1B2. Therefore, the error will not appear when intercepting the reflectors at surface but will become apparent in boreholes, or when attempting to match in depth reflectors from crossing profiles. The geometrical relation between segments A1A2 and B1B2 depends only on the slant of the segment A1A2 in the X-t representation and the velocity. B1B2 can therefore be computed without reference to the possible out-of-vertical position of B1B2. The locus of B1B2 is a conical sheet with its axis along the measuring line.

Velocity field and reflector positioning

The figures from Section 4.1.5 of R-02-43 contain an "approximate depth" axis which is derived from the time axis and a constant velocity V=5,850 m/s. Firstly, let us note that "depth" should not refer to "vertical depth", but to the distance from the measuring line, as explained in the section above. Secondly, a discussion is needed to determine whether 5,850 m/s is indeed the constant velocity value providing the minimum estimation error in depth. Figure A1-2 below is drawn based on Figure 4-19 of R-02-43 and presents the estimated average variation of the velocity with the depth.

Two-way travel times have been computed vs. depth for the velocity model of Figure A1-2, for V=5,850 m/s and for V=6,000 m/s with a 4 ms delay. This delay would be introduced by the low velocity zone between 0 m and 150 m depth. The aim is to minimize the errors in estimating the actual depth of the reflectors introduced by the use of constant velocity, with respect to the "true" depth computed by the variable velocity model. Of course, the meaning of "true" is relative, depending on how accurate the variable velocity model is and on how inclined the path to any given reflector is with respect to the vertical depth. The velocity

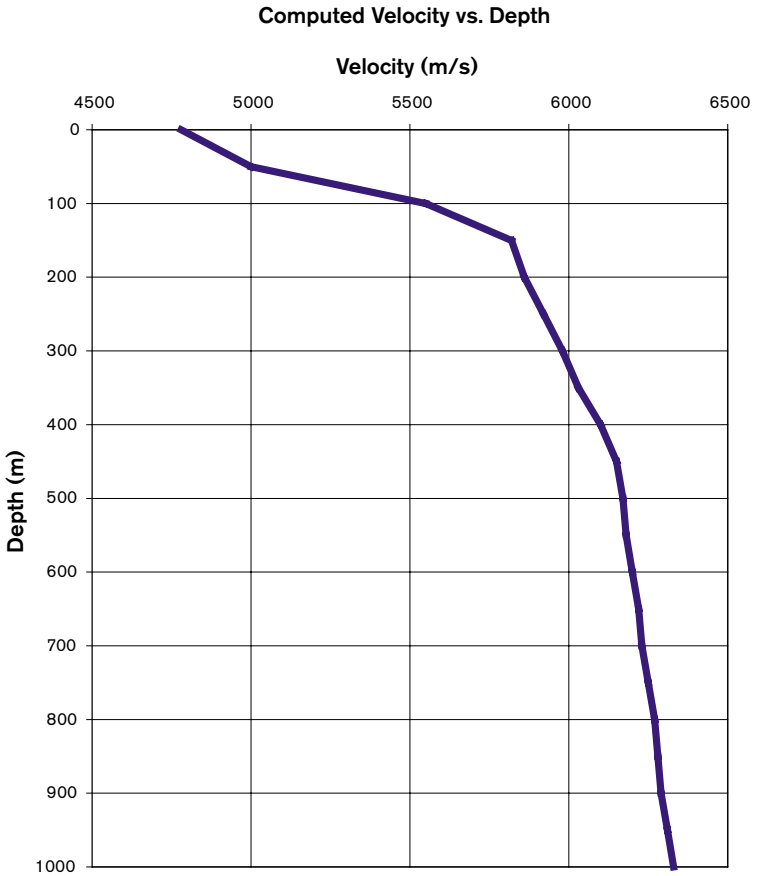

Figure A1-2. *Computed velocity vs. depth (cf. Figure 4-19 of /Juhlin et al. 2002/).*

model is likely to be sufficiently accurate through most of the site, as proven by the velocity analysis performed in Section 4.2 of R-02-43. Likewise, the velocity variations at depths over 150 m is relatively small and therefore the errors possibly induced by non-vertical reflection paths is likely to be within approximately +/– 12 m, i.e. less than +/– half of a wavelength. The introduction of an additional delay to compensate for the near surface low velocity will distort events from reflectors shallower than 150 m, which are not interpretable anyway, but will reduce the errors in estimating the depth of deeper reflectors. This point is proven in Figure A1-3, which presents the depth error vs. depth, relative to the "true" velocity model, for V=5,850 m/s (magenta) and for V=6,000 m/s, with 4 ms delay (yellow). The latter approximation is clearly better, as it brings the errors at any depth to within +/– 12 m, i.e. to less than +/– half of a wavelength.

The Crux Point method

Seismic reflection profiles are two-dimensional distance-time representations. Even after transforming the X-t axes into X-R axes, as described above, a reflecting plane cannot be fully determined from a single 2D profile. What can be determined is the relative slope of the reflector with respect to the acquisition line (assuming that the line is straight). The reflection on a plane will occur along a line segment, with the reflector plane being perpendicular to the plane formed by this segment and the measuring line. The non-determination when going from 2D to 3D will turn the locus of the reflection segment into a conical surface having the measuring line as its axis. Determining fully the position of a reflector from two or more profiles could then be done by finding a plane, which is tangent to several conic surfaces with axes oriented differently in space. However, one may find this procedure quite cumbersome in practice and a more user-friendly approach has been used here.

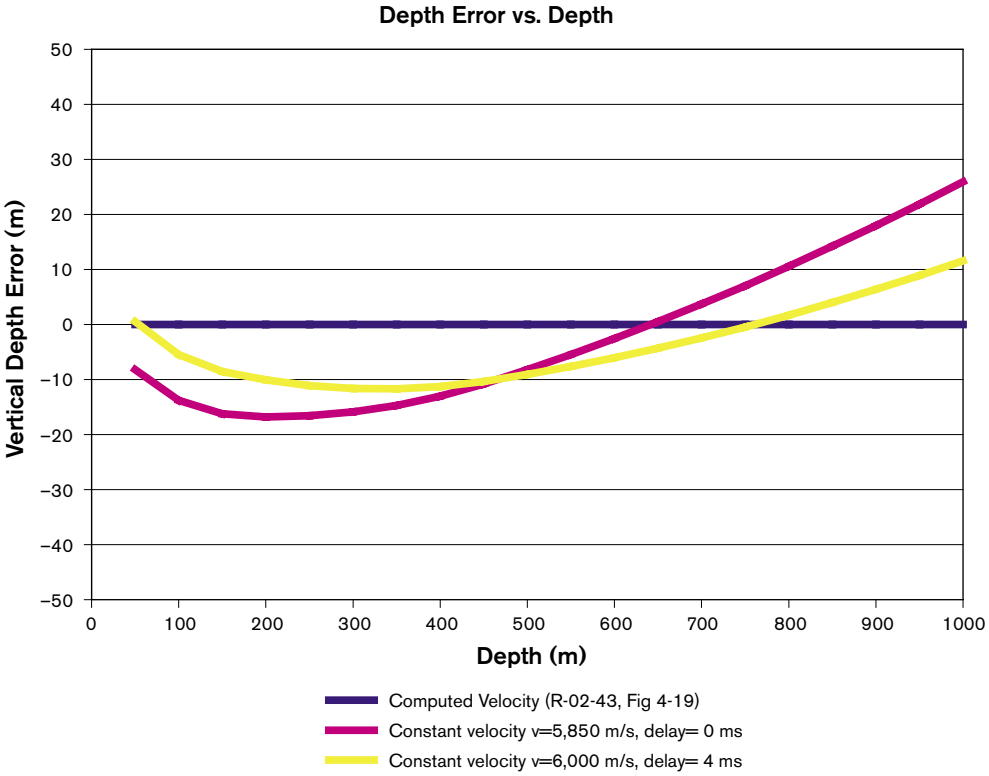

Figure A1-3. *Depth error relative to the computed variable velocity model for V=5,850 m/s and V=6,000 m/s with 4 ms delay.*

The “Crux Point” of a plane is defined as the foot of the perpendicular descended on a plane from a chosen origin. The locus of the Crux Point of a reflector appearing as a line segment in a 2D profile is a curve in space, rather than a conical surface. The best-fit plane solution for the reflector is found at the intersection of the Crux Point loci. If all profiles are horizontal and on ground surface, there will be two mathematical solutions, symmetrical with respect to the ground surface. Obviously, the solution up in the sky can be neglected. Estimating interactively the intersection of Crux Point curves is far easier than the common tangent plane to conical surfaces, which makes the Crux Point method more tractable.

Once the plane of the reflector has been determined by the Crux Point match, the positions of the reflection segments along the reflecting planes corresponding to the events observed in the data profiles can be calculated. In practice, however, depicting reflectors by line segments is not completely suggestive to the viewer. The reflecting segments are therefore represented as plane elements with a transverse dimension of roughly to 3–4 signal wavelengths.

The Crux Point method is exemplified in Figure A1-4. One can notice the intersection of the crux point loci determining the position and orientation of the reflector plane (red dot) and the alternative “up in the sky” solution, which was discarded. The second red dot, near the investigation lines at ground surface, is the crux point origin, common for all profiles. The actual reflector elements corresponding to the three profiles are also presented.

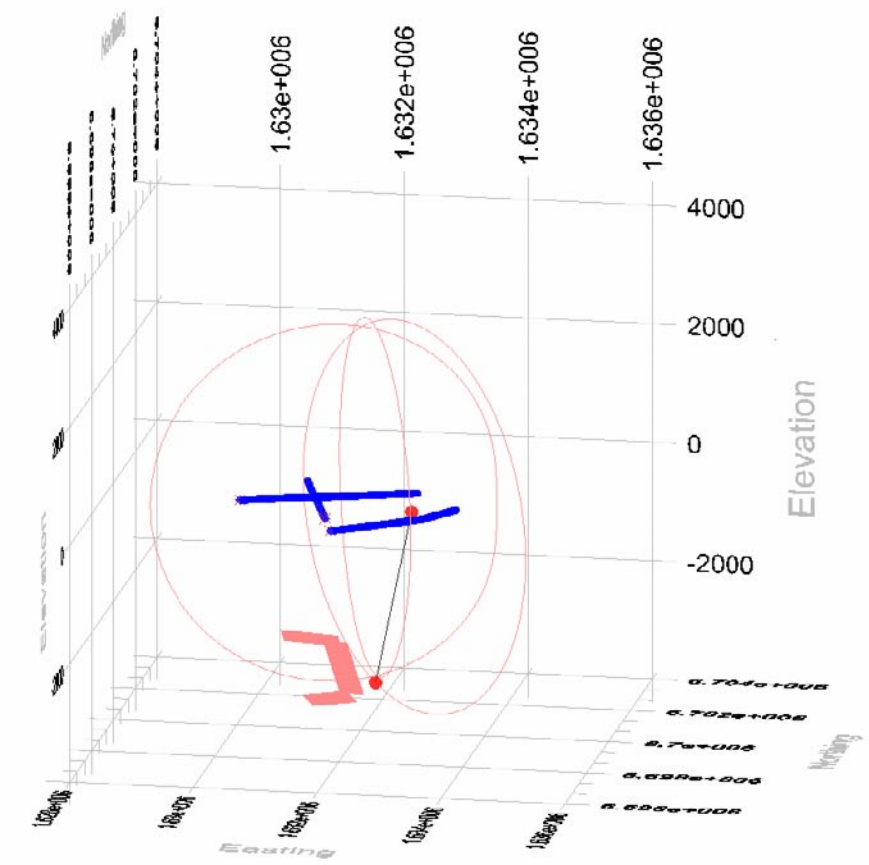

Figure A1-4. *Crux Point definition and reflection elements for three surface profiles.*

Appendix 2

Seismic profiles

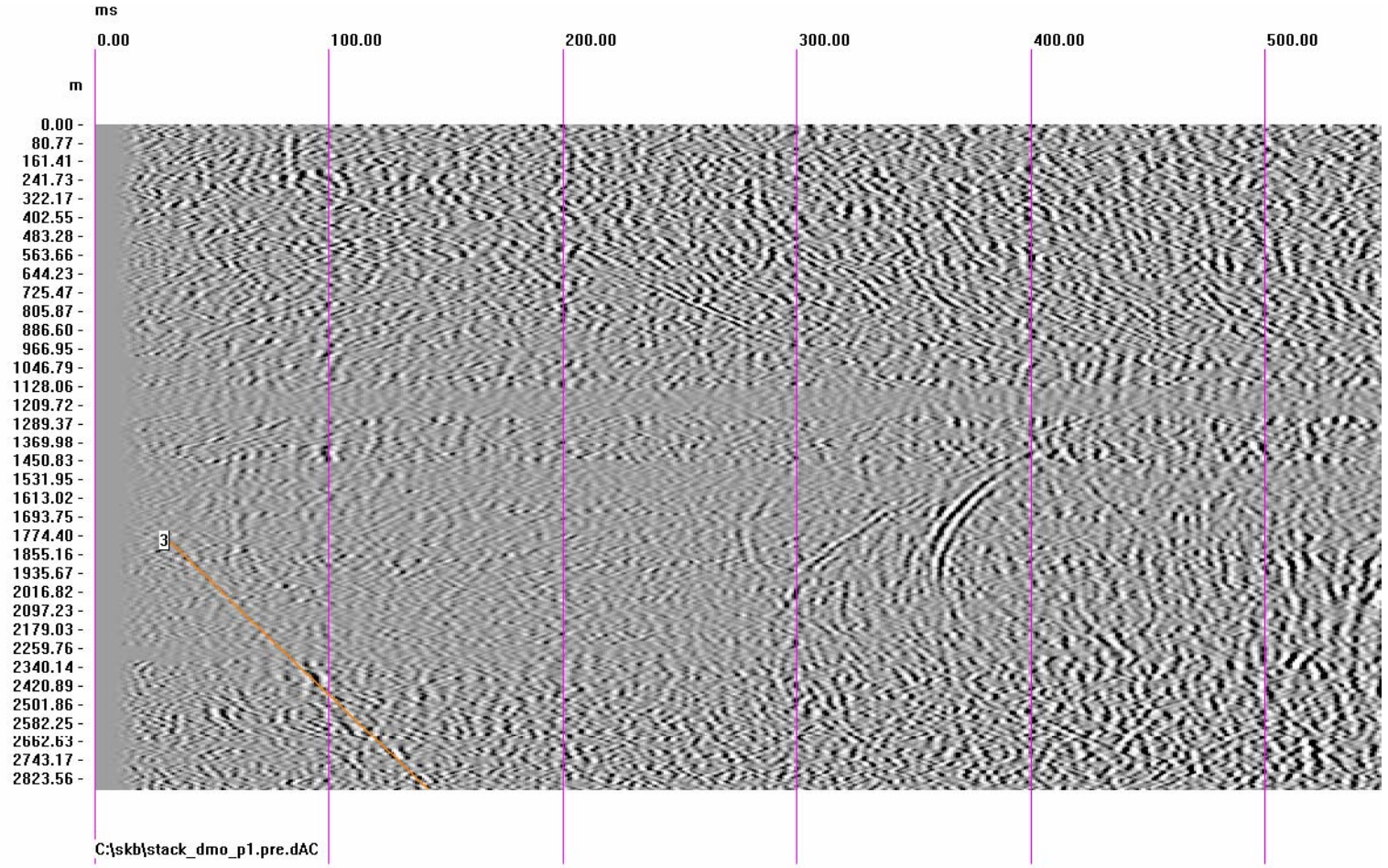

Figure A2-1. *Profile 1 reflector B7 (3).*

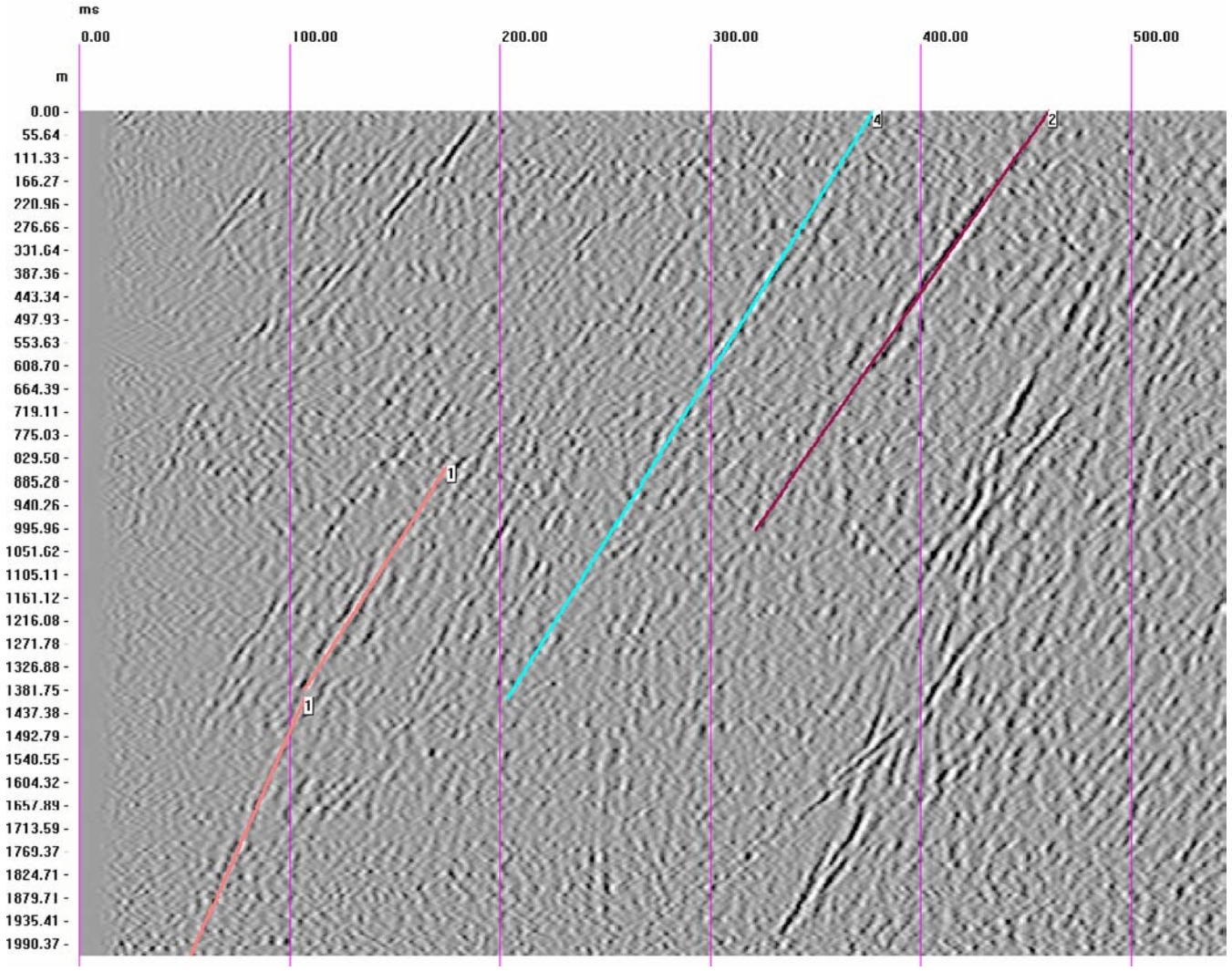

Figure A2-2. *Profile 3, reflectors A7 (1), B6 (2), A3 (4).*

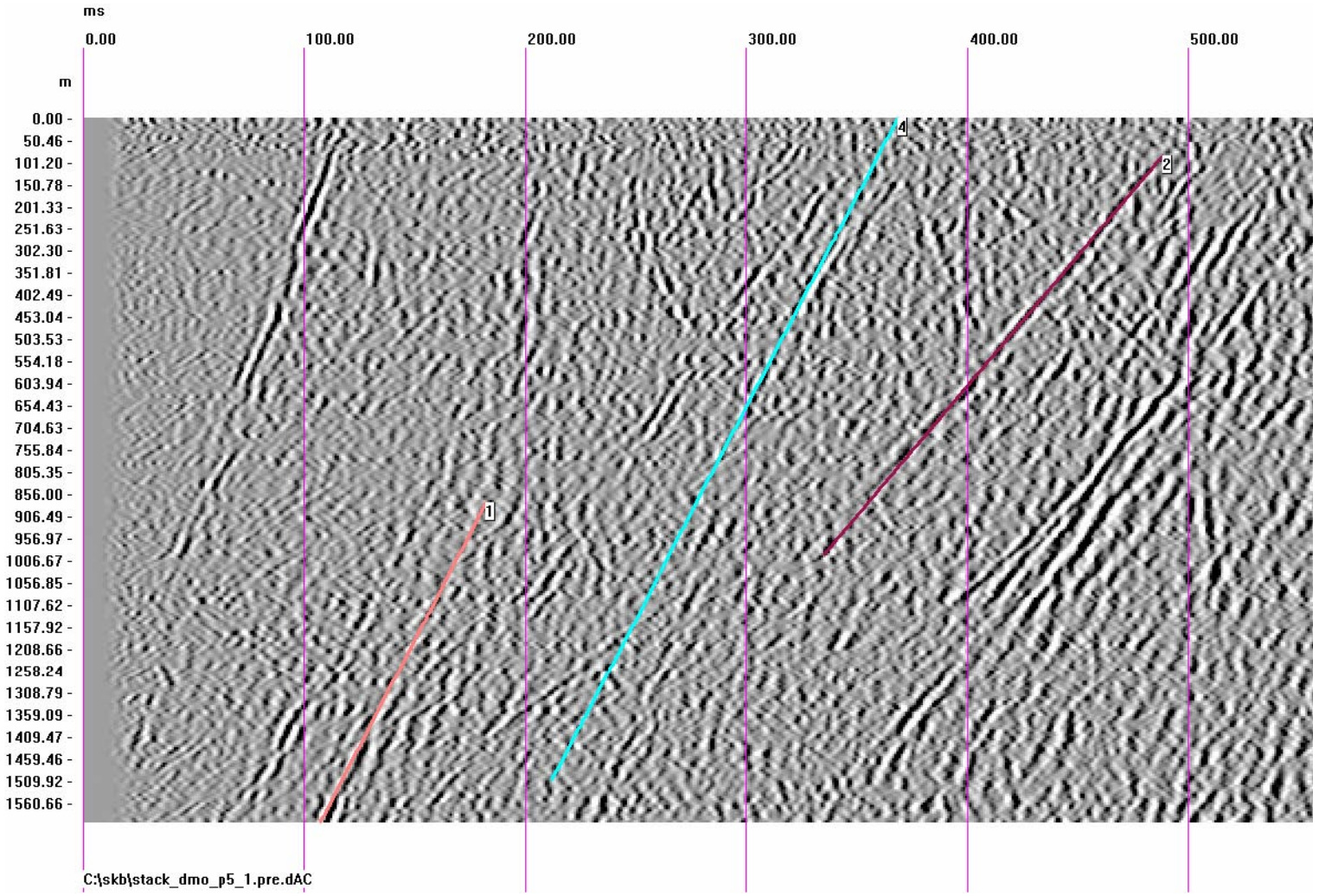

Figure A2-3. *Profile 5.1, reflectors A7 (1), B6 (2) and A3 (4).*

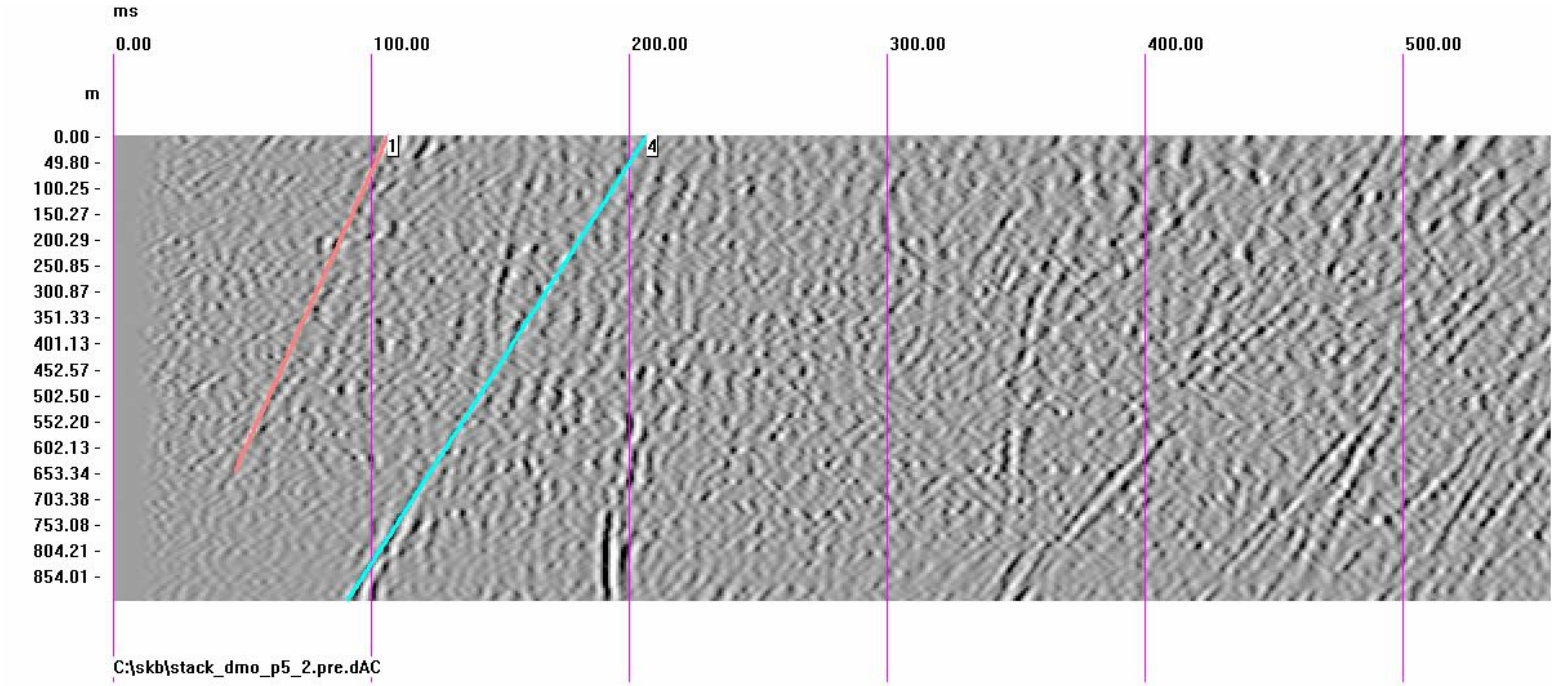

Figure A2-4. *Profile 5.2, reflectors A7 (1) and A3 (4).*

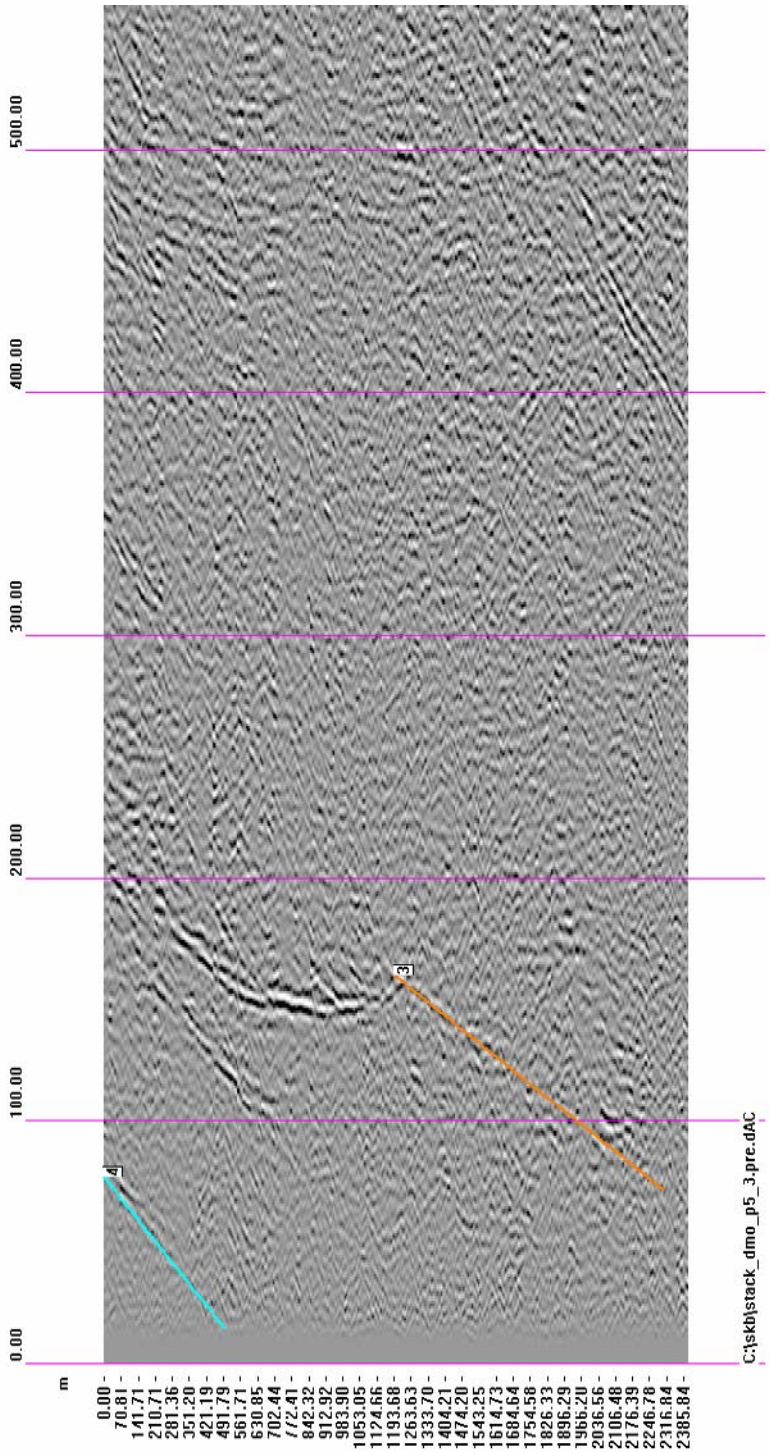

Figure A2-5. *Profile 5.3, reflectors B7 (3) and A3 (4).*